DESY 80/76
July 1980

First Results from the PETRA-Polarimeter

by

H.D. Bremer, H.C. Dehne, H.C. Lewin, H. Mais,
R. Neumann, R. Rossmanith, Rüdiger Schmidt

I. INTRODUCTION

In electron-positron storage rings beam gets vertically polarized by the synchrotron radiation [1] but various depolarization mechanisms can have an adverse effect on polarization: the build-up time for the polarization is given by the formula:

$$P = P_\infty \, (1 - e^{-t/\tau})$$

wherein P is the degree of polarization

τ is a combination of two time constants

$$\frac{1}{\tau} = \frac{1}{\tau_{Dep}} + \frac{1}{\tau_{pol}}$$

with $\tau_{pol} = 98 \, \frac{R^3 \, \{m\}}{E^5 \, \{GeV\}} \, \frac{<R>}{R}$

and τ_{Dep} ..... depolarization time constant

R = bending radius of the storage ring magnets

$<R>$ = average radius of the storage ring

E = energy of the stored beam

$$P_\infty \, (\%) = 92 \, \frac{1}{1 + \frac{\tau_{pol}}{\tau_{Dep}}}$$

The spins of the individual particles precess around the vertical bending field of the storage ring. The precession frequency depends on the energy of the particle. Thus it is only the vertical component of the spin which is stable over many revolutions. Depolarization resonances are expected when a perturbating field rotates the vertical polarization through many revolutions into the horizontal plane where polarization is lost. For time independent perturbation fields the strongest depolarization resonances are expected at the following energies:

$$\frac{g - 2}{2} \gamma = n \pm m Q_z$$

γ = energy of the electron/rest energy of the electron
g = anomalous part of the electron magnetic moment
n = Integer; $m = 0, \pm 1$
Q_z = vertical Q-value of the storage ring

The width of these resonances is usually calculated by computer programs [2], but each calculation can only describe a real storage ring to a limited extent.

With the PETRA polarimeter it is possible for the first time to compare theory and experiments in a storage ring the size of PETRA (beam energies between 5 and 19 GeV, circumference 2.3 km). The results of polarization measurements in other storage rings are summarized e.g. in [3]. The PETRA-polarimeter is described more detailed in [4]. The basic idea is the following: circularly polarized photons are fired against the electron beam. In the case of vertical electron beam polarization a different number of photons is scattered into the upper and the lower half plane. By detecting the differences in the number of photons between the two half planes, the degree of the polarization of the electron beam can be determined.

Fig. 1 shows the principal arrangement of the polarimeter: The Ar^+-laser emits a green light pulse when an electron bunch approaches the quadrupole. The vertically polarized laser pulse is converted by a Pockels-crystal into circularly polarized light and meets the electron bunch in the vacuum chamber via two mirrors. The helicity of the photon beam depends on the sign of the high voltage applied on the Pockels-crystal and can simply be altered by changing the high voltage. Some of the laser photons are converted by the electron beam into high energy photons. The high energy photons travel with the electron beam up to the first weakly excited bending magnet, leave the electron beam in this bending magnet and leave the vacuum chamber in the following bending magnet and enter the detection system 45 m from the point where they are generated.

The detection system consists of a combination of counters (fig.2). Since vertical asymmetries in the counting rates have to be detected, the heart of the detector is a vertically movable converter between an assembly of counters. The veto counters suppress the charged particles generated outside the detector and the trigger counters trigger the electronics when a photon in the converter plate (a tungsten plate with a height of 1 mm) is converted. A shower counter at the end of the detector measures the energy of the photon. The high energy background is reduced by moving vertical beam bumps as described in detail in [4].

II. The Alignment and the Calibration of the Polarimeter

Fig.3 shows the measured spectrum of the backscattered photons. Each energy corresponds to a certain scattering angle α (fig.4). Photons being scattered in the direction of the electron momentum have the maximum possible photon energy, photons being scattered under a scattering angle α have the less energy the larger the angle α is.

In the spectrum (fig.3) two different energy regions are marked. In the one region the photons with the highest possible energy are included (in the following called high energy photons) and in the second region the photons emitted under the angle $\alpha \approx 1/\gamma$ (in the following called medium energy photons). As mentioned in the introduction more photons are scattered into the upper or lower half plane than into the other in the case of electron beam polarization: this statement is valid for medium energy photons. For high energy photons the asymmetry is relatively small.

In fig.5 the superposition of this effect with many particles is illustrated; assuming there are two parallel flying electrons (5a) then the medium energy photons superimpose in such a way that the absolute value of the asymmetry is smaller than in the case of fig. 5b. In this case the two electrons travel on convergent trajectories.

As a result of these considerations the electrons have to be illuminated at a position where the convergence of the electron beam enables the detection of the maximum asymmetry. In the quadrupole where the photon beam and the electron beam interact, the convergence of the electron beam varies so that the correct interaction point has to be adjusted by moving a remotely controlled mirror. The correct interaction point is found by using horizontally polarized light (light polarized in the plane of the storage ring) instead of circularly polarized light. For horizontally and circularly polarized light the photons belonging to the high energy part of the spectrum are emitted into the direction of the electron trajectory. If integration is done over the horizontal direction (this is done by the movable converter) the medium energy photons generated by horizontally polarized light are emitted into the upper and lower halfplane as demonstrated in fig. 6. The emission probability in the direction of the electron trajectory is at a minimum.
Fig. 7 shows the measured vertical photon distribution when the electron beam is illuminated near the correct interaction point. The dip in the middle of the medium energy range photons demonstrates that photons emitted into the upper plane are measured by the detector at the upper plane and vice versa.

III. First Measurements of Polarization in PETRA

The polarization of the electron beam is measured by using a circularly polarized photon beam. The calculated vertical beam profile for 100 % electron beam polarization and right and left-handed circularly polarized light is shown in fig. 8. From this figure it is evident that the polarization measurements can be carried out in two different ways:

a) half of the profile is shadowed off by an absorber and the difference in the counting rates between left and right handed photons is measured

$$V_a = \frac{n_R - n_L}{n_R + n_L}$$

b) the difference in the counting rates between left and right handed photons is measured as a function of the converter position.

It is evident that for precise measurements method b) is the more accurate but method a) can be used for faster measurements. The advantage of method b) is the following:

The circularly polarized laser beam has in general a small content of linear polarized light. This linear polarization alters the profiles in fig. 8. The influence of the linear polarization can be eliminated by calculating the following value

$$V_b = \frac{1}{2}\left(\frac{n_R - n_L}{n_R + n_L}\right)_{z = a} - \frac{1}{2}\left(\frac{n_R - n_L}{n_R + n_L}\right)_{z = -a}$$

n_R measured counting rate for right handed photons
n_L measured counting rate for left handed photons
$( )_{z = a}$ measured at the vertical position a
$( )_{z = -a}$ measured at the vertical position -a

Fig. 9 shows two different tests for beam polarization: the calculated difference in the counting rate for 100 % polarization is compared with the measured V-values. At 15.3 GeV the polarization of the electron beam is either very small or non-existent and at 15.2 GeV the electron beam is polarized up to about 40 % (±10 %).
Both curves were measured under the following conditions:

a) The beam energies were 15.2 resp. 15.3 GeV. The expected depolarizing resonances are shown in fig. 10.
b) The vertical beta in the interaction region was 140 cm.
c) The machine was only filled with electrons.
d) The feedback system was out of operation.
e) The solenoids of the experiments were switched off.

At 15.3 GeV the beam polarization is destroyed by the depolarizing resonance

$$\frac{g-2}{2}\,\gamma = 58 - Q_z$$

This measurement was repeated about four and eight weeks later and similar results were obtained. This clearly proves that machine conditions can be found in PETRA where reproducible beam polarization can be obtained.

For luminosity runs the vertical beta in the interaction region is not 140 cm as in the above mentioned measurements but about 20 cm (so called M 20 optics). On a few occasions polarization measurements using these optics were carried out at the following energies: 11.2, 13.86, 17.4 and 17.5 GeV. Beam polarization was not observed atany of these energies. The data from the measurements at 13.86 GeV are published[5]. A comparison of the degree of polarization between these two optics under the same conditions (the same energy and the same Q-values) has not been made up to now. These measurements and a study of the influence of the beam-beam effect on the degree of the polarization will be one of the aims of future measurements.

IV. Fast depolarization by time-dependent magnetic fields

In order to destroy the beam polarization without changing the energy a fast depolarizing device was installed. The basic idea is as follows: as mentioned in the introduction polarization can be destroyed by fields acting on the spin in the same direction over many revolutions. If the storage ring is not working on depolarizing resonances this is only possible with time-dependent perturbating fields. Thus, for example horizontal magnetic fields with the frequency ν_{pert}

$$\left(\left(\frac{g-2}{2}\right) \gamma - m \right) \cdot \nu_o = \nu_{pert}$$

ν_o ..... revolution frequency of the beam

m = integer part of $\frac{g-2}{2}\,\gamma$

can destroy polarization.

A sweep generator was connected to the vertical PETRA feedback system. The central frequency of the sweeper was tuned to the value for ν_{pert} calculated from the usual energy indicator of PETRA. This energy value is calculated by the magnetic field strength. The sweep was ± 10 KHz from this central frequency. The results are shown in fig. 11. The polarized electron beam becomes depolarized within a relatively short time after the depolarizer was switched on and remains depolarized. The residual asymmetry in the case of complete depolarization is due to the fact that the measurement was carried out with method a) and as a consequence an elimination of the linear component is not possible. After the depolarizer has been switched off the polarization builds up again.

With this method a calibration of the beam energy is possible. According to the above mentioned figures one can estimate that the energy calibration is within ± 0,3 % of the energy calculated by the magnetic field. This figure is preliminary and an exact measurement of the absolute energy will also be an aim of future investigations.

V. Summary

With the PETRA polarimeter electron beam polarization was detected. Up to now the polarization was only detected under certain machine conditions, e.g. without beam-beam interaction. The aim of the future measuring program will be to find out which parameters are decisive for the polarization.

VI. Acknowledgements

The authors wish to thank Prof. Dr. G.A. Voss for many suggestions, Dr. A. Chao from PEP for sending us the spin simulation programm SLIM and for many very helpful discussions, Mr. J. Kewisch and Dr. Ripken for their help in programming, Mr. Cirsovius, Mr. Grell, Mr. Höhse and Mr. Pätzold for installing the digital data handling system for the polarimeter and Mr. Fischer and Mr. Sarau for the development of the vacuum mirrors.

VII. Literature

1) V.N. Baier
XLVI Corso International di Fisica "Enrico Fermi". 1969
Academic Press, New York 1971

2) A.P. Chao
IEEE Trans. Nuclear Sc.
Vol. NS-26, No. 3, (1979), 3482

3) R.F. Schwitters
Conference Proc. AIP No. 51
High Energy Physics with Polarized Beams and Targets, p.91

4) Rüdiger Schmidt:
Aufbau und Test des Polarisationsmonitors an PETRA
DESY M 80-04

5) D. Degele et al.:
Results on Machine Physics Studies on PETRA in 1979,
DESY 80/10

VIII. Figure Captions

Fig. 1: The polarimeter

Fig. 2: The detector assembly

Fig. 3: The spectrum of the scattered photons measured with the showercounter. Two different energy regions (the so called high energy and the medium energy region) are marked (electron energy 15.2 GeV).

Fig. 4: The energy of the scattered photons depends on the scattering angle α. The maximum energy is achieved when the electron is scattered in the direction of the electron trajectory ($\alpha = 0$).

Fig. 5: Demonstration that the maximum asymmetry effect is achieved at the detector when a convergent electron beam is illuminated by the laser beam (fig.5b). For a parallel particle beam the asymmetry effect is reduced (fig.5a).

Satzspiegel

Fig. 6: Emission probability for the back-scattered photons when the incoming laser light is polarized perpendicular to the paper plane. If integration is done over the horizontal direction (this is done by the movable converter) the high energy photons are scattered in the direction of the electron trajectory, the medium energy photons have a minimum emission probability in the direction of the electron trajectory.

Fig. 7: The vertical profile of the back-scattered photons for "high" energy and "medium" energy photons. The light is polarized in the plane of the storage ring. The profile of the medium energy photons has a dip in the middle. The reason for the dip is explained in fig. 6. When the dip is seen it is clear proof that the electron beam is illuminated near the focal point: photons emitted at the interaction point into the upper half plane arrive at the detector at the upper half plane and vice versa.

Fig. 8: Expected vertical profile for a 100 % vertically polarized electron beam. The photon beam is circularly polarized. The two curves relate to different helicities of the laser beam.

Fig. 9: Difference in counting rates between right and left-handed circularly polarized light (asymmetry) as a function of the position of the converter. The solid line shows the expected difference for 100 % beam polarization. Both the measured points for V_b and a fit is shown. The fit was done in the following manner: the ratio $(n_R - n_L)/(n_R + n_L)$ was measured as a function of the vertical position Z. Through these measured points two extremal curves and a curve in between these two curves were fitted. Along these three fitted curves the value for V_b was calculated leading to the three curves of this figure at 15.2 GeV. For 15.3 GeV only the positive V values are shown since negative V values cannot exist.

Fig. 10: Possible depolarizing sources near to the energy where the polarization measurements were carried out (Q_x = .2 , Q_z = .3 , Q_s = .08).

Fig. 11: The beam is depolarized by a fast depolarizing device (beam energy 15.2 GeV). After switching off this device the polarization builds up again.
The measurements were done by method a):
the residual linear polarization of the laser beam causes a residual V-value even when the beam is completely depolarized.

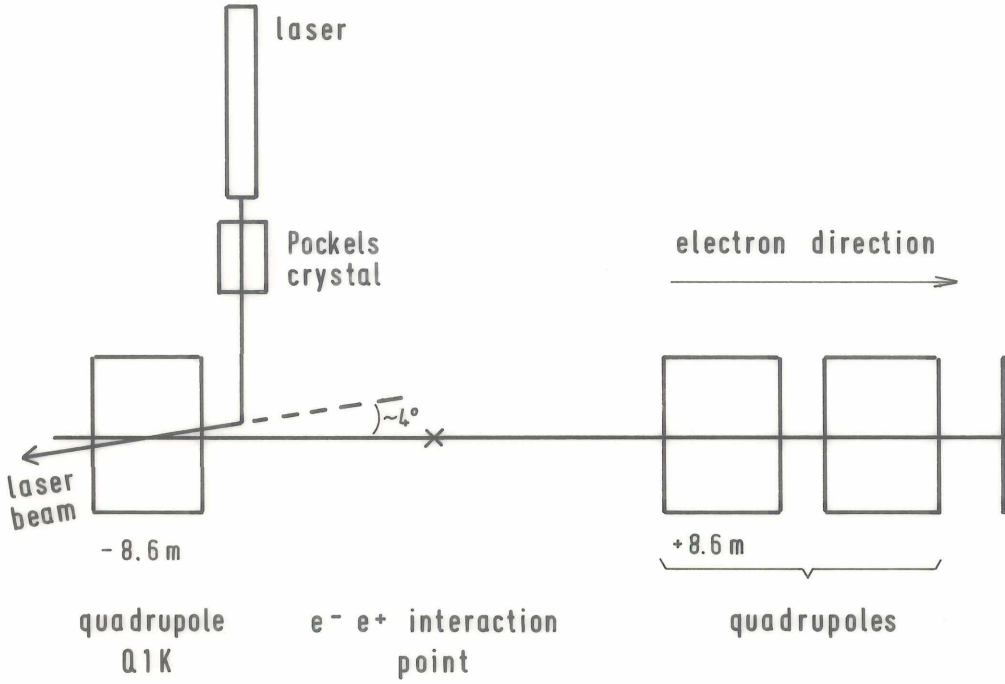
laser
Pockels crystal
electron direction
~4°
laser beam
- 8.6 m
+ 8.6 m
quadrupole Q1K
e⁻ e⁺ interaction point
quadrupoles

fig. 1

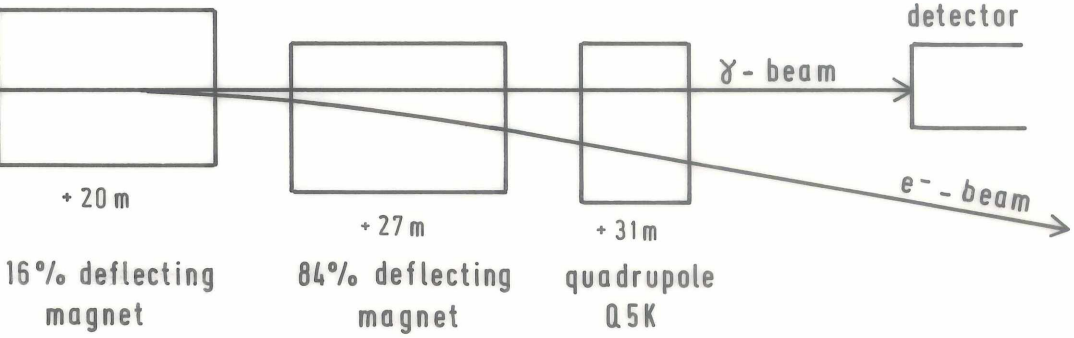
detector
γ - beam
e⁻ - beam
+ 20 m
+ 27 m
+ 31 m
16% deflecting magnet
84% deflecting magnet
quadrupole Q5K

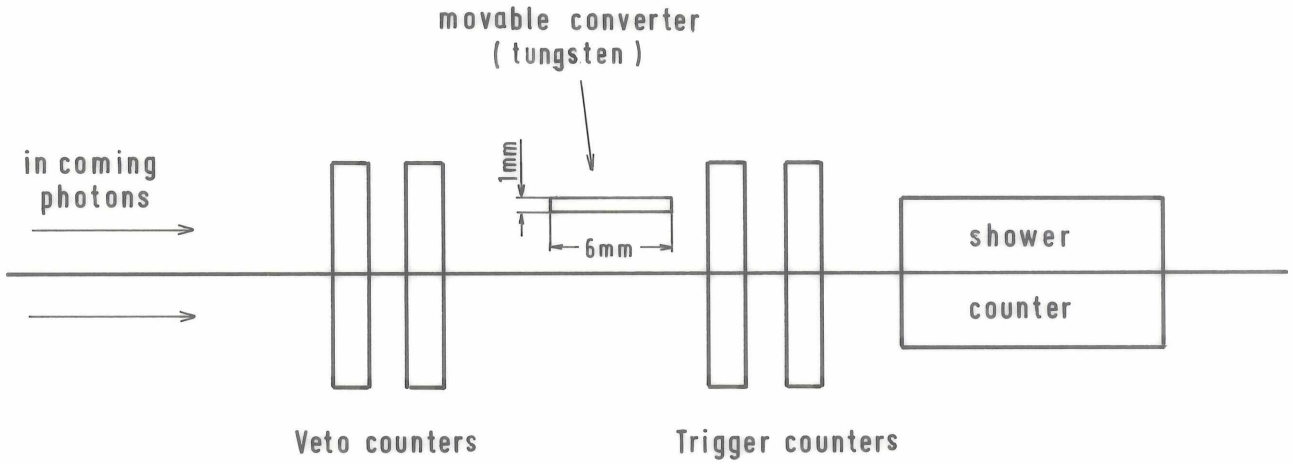
movable converter
(tungsten)
in coming
photons
1mm
6mm
shower
counter
Veto counters
Trigger counters

fig. 2

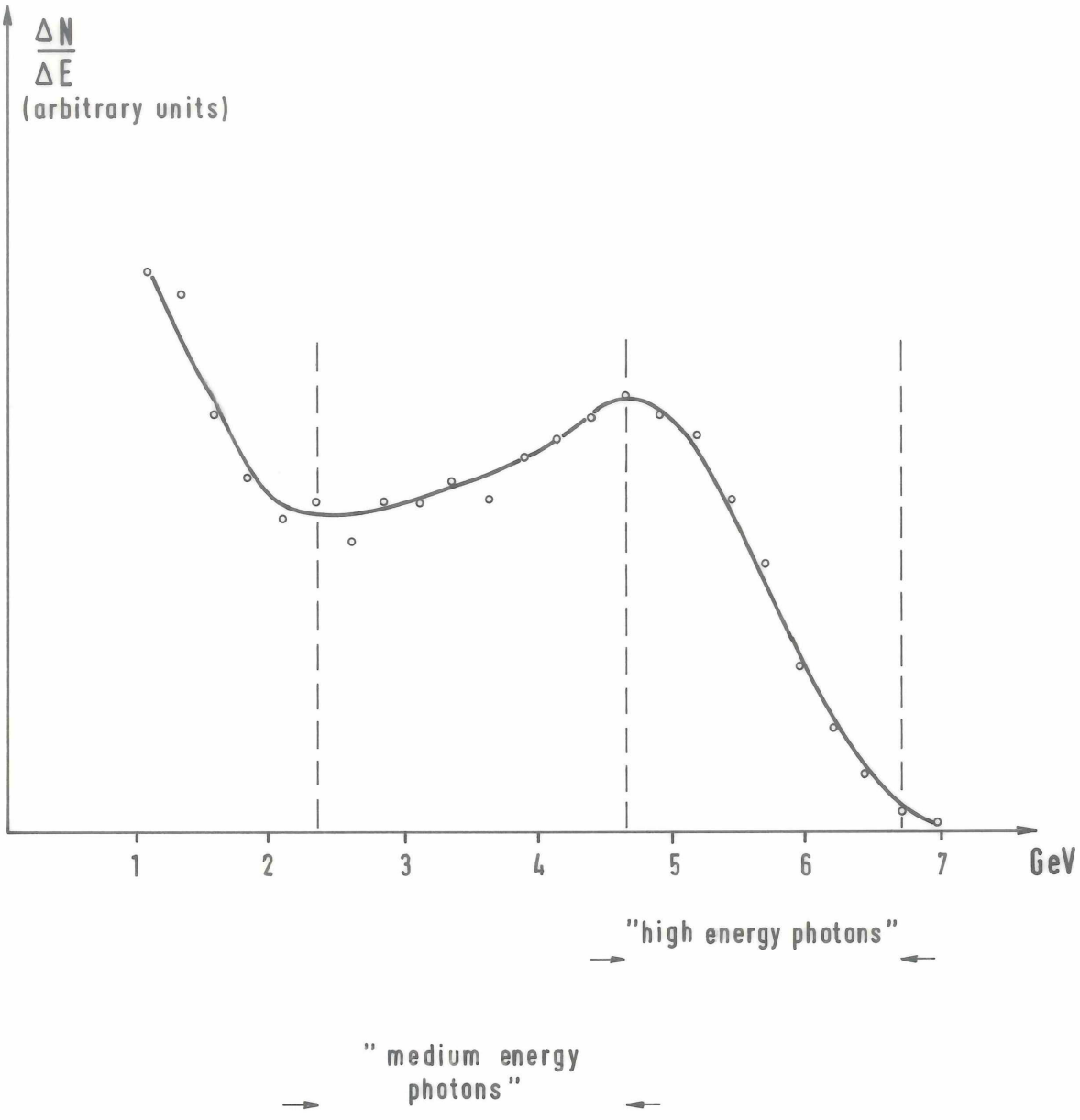
ΔN/ΔE
(arbitrary units)
1
2
3
4
5
6
7
GeV
"high energy photons"
" medium energy photons"

fig. 3

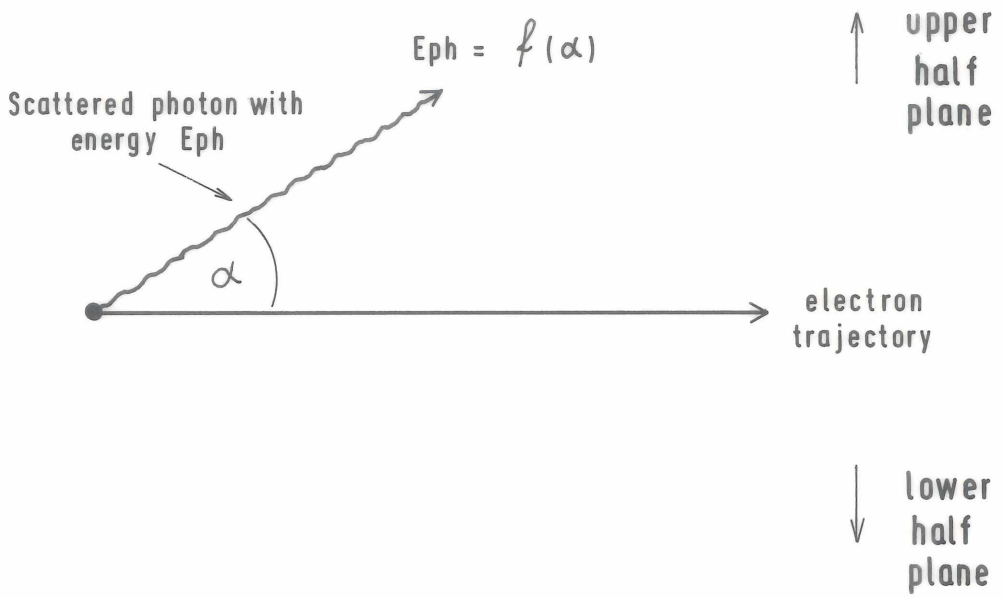
Eph = f(α)
upper
half
plane
Scattered photon with
energy Eph
α
electron
trajectory
lower
half
plane

fig. 4

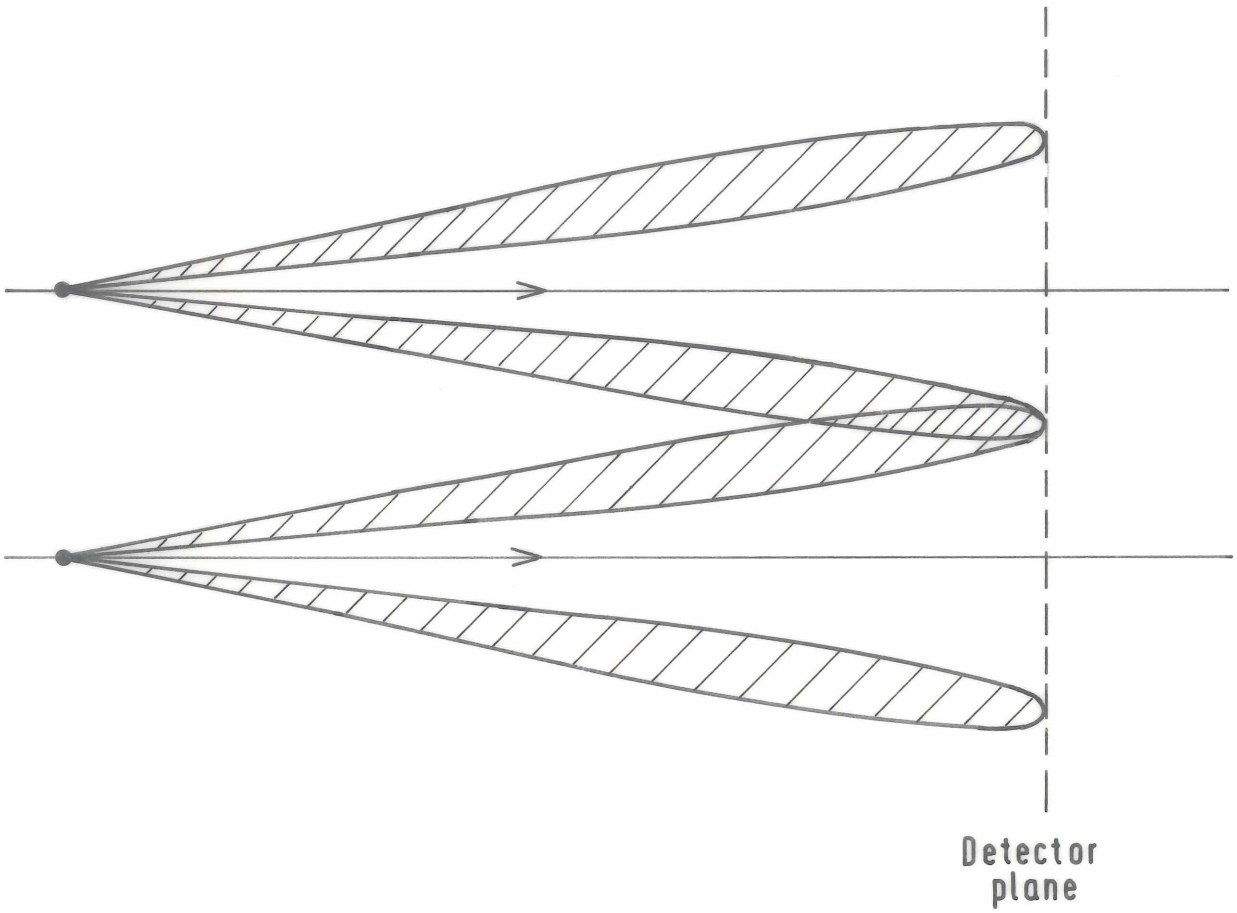

fig. 5a

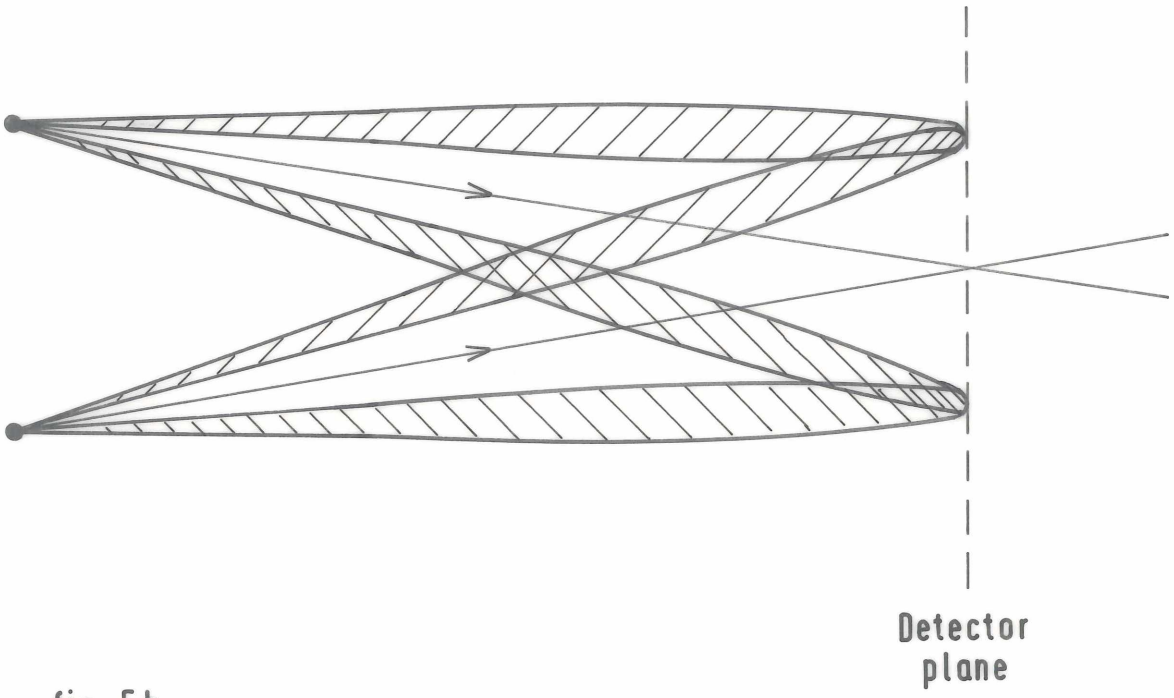

fig. 5 b

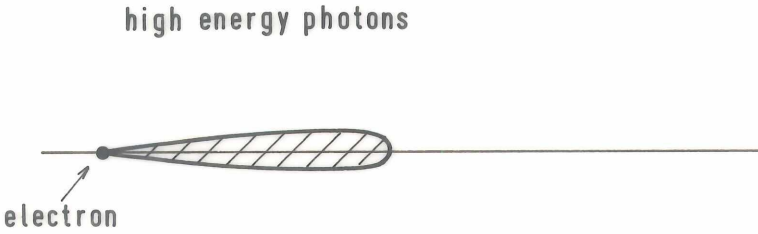

fig. 6a

Fig. 6

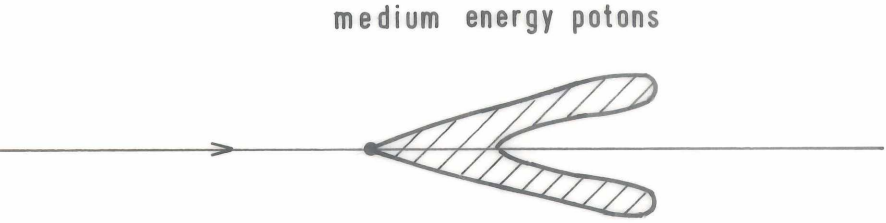

fig. 6 b

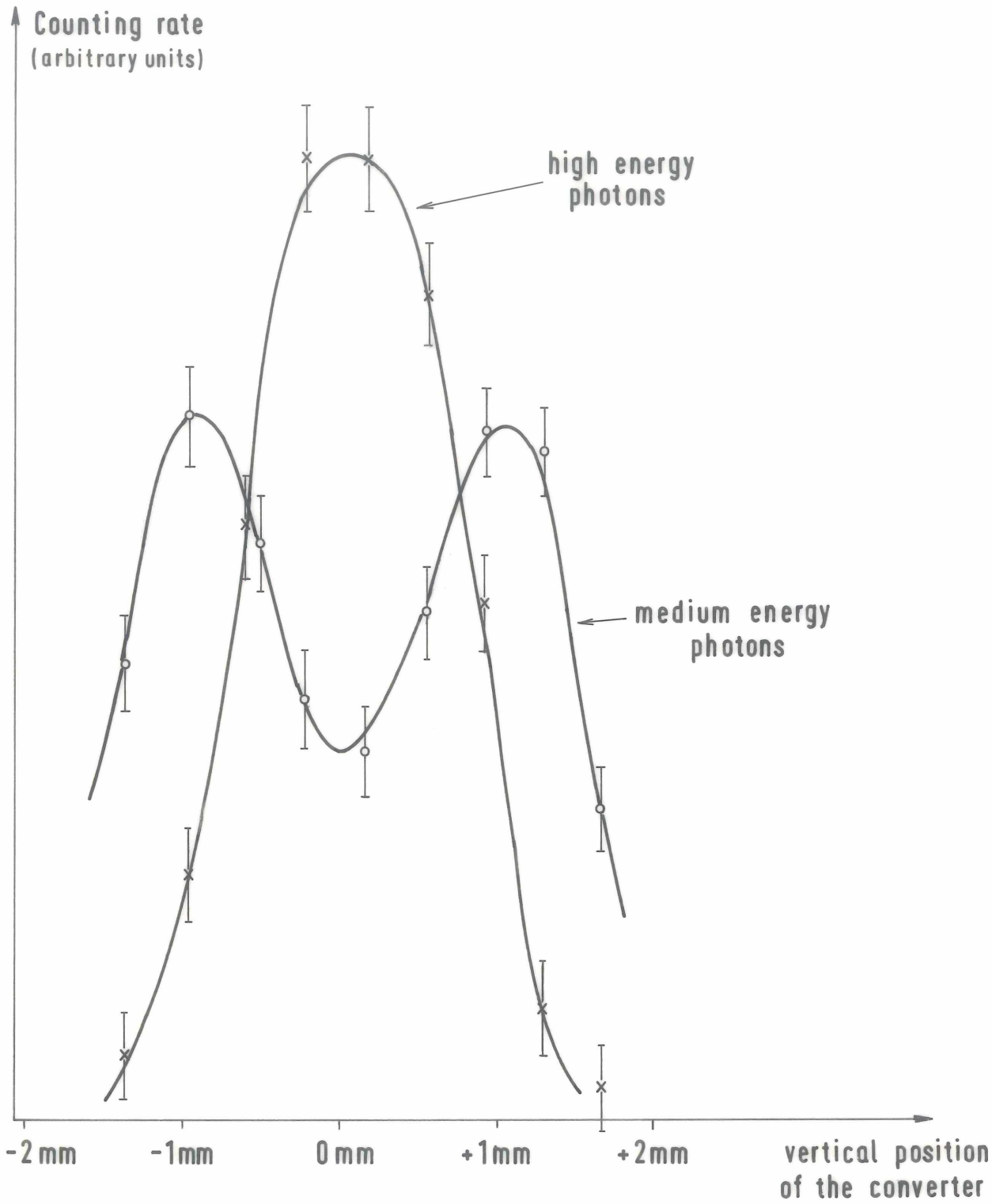
Counting rate
(arbitrary units)
high energy
photons
medium energy
photons
-2 mm
-1mm
0 mm
+1mm
+2mm
vertical position
of the converter

fig. 7

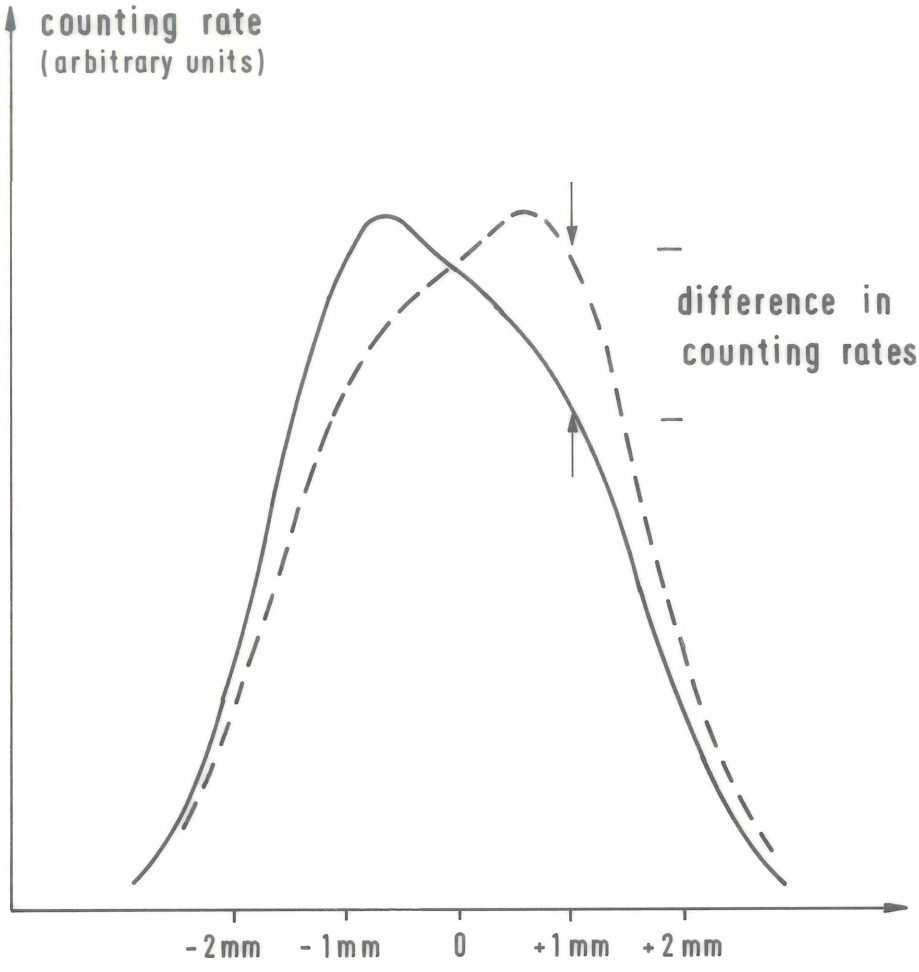
counting rate
(arbitrary units)
difference in
counting rates
-2mm
-1mm
0
+1mm
+2mm

fig. 8

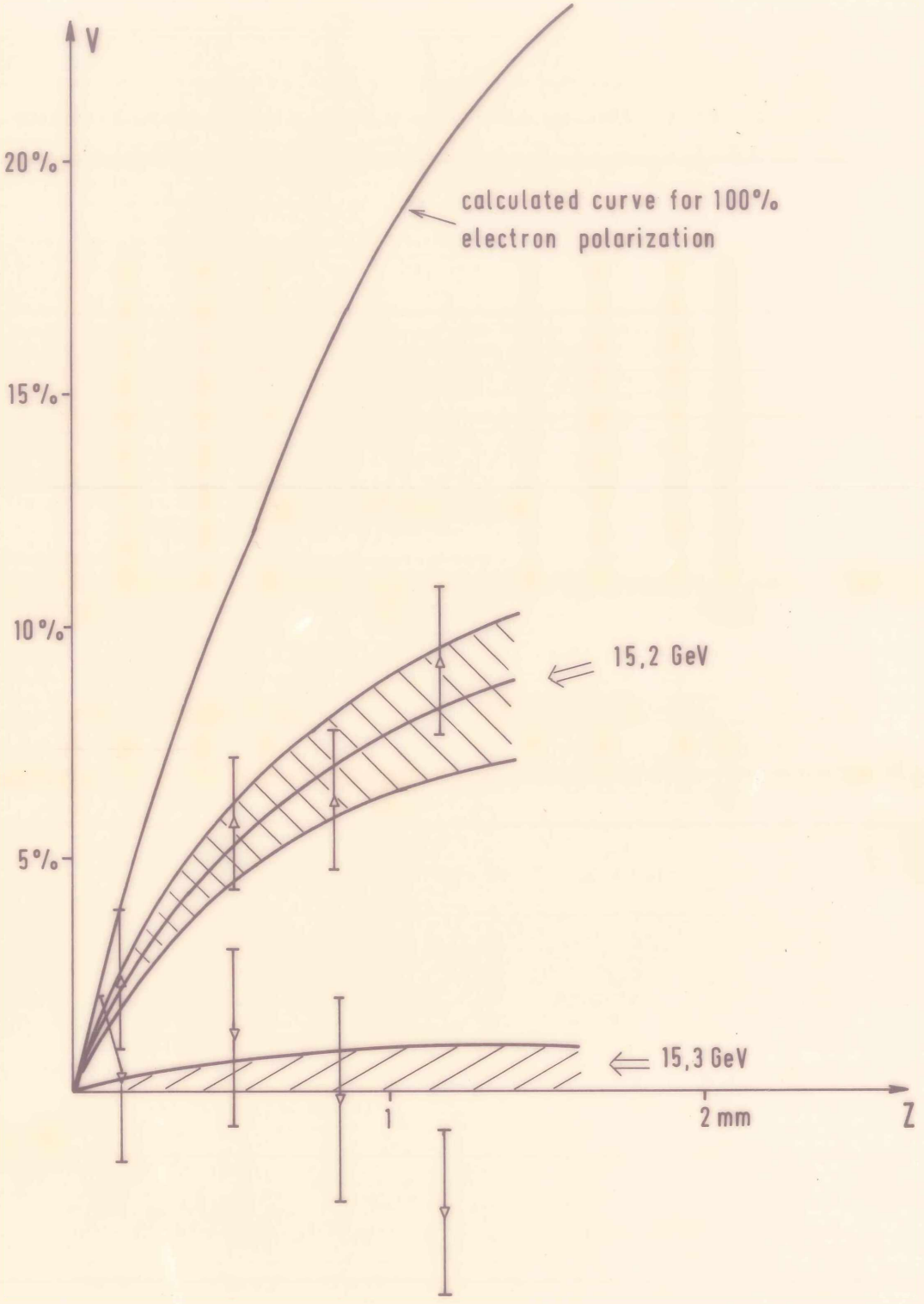
V
20%
15%
10%
5%
calculated curve for 100%
electron polarization
15,2 GeV
15,3 GeV
1
2 mm
Z

fig. 9

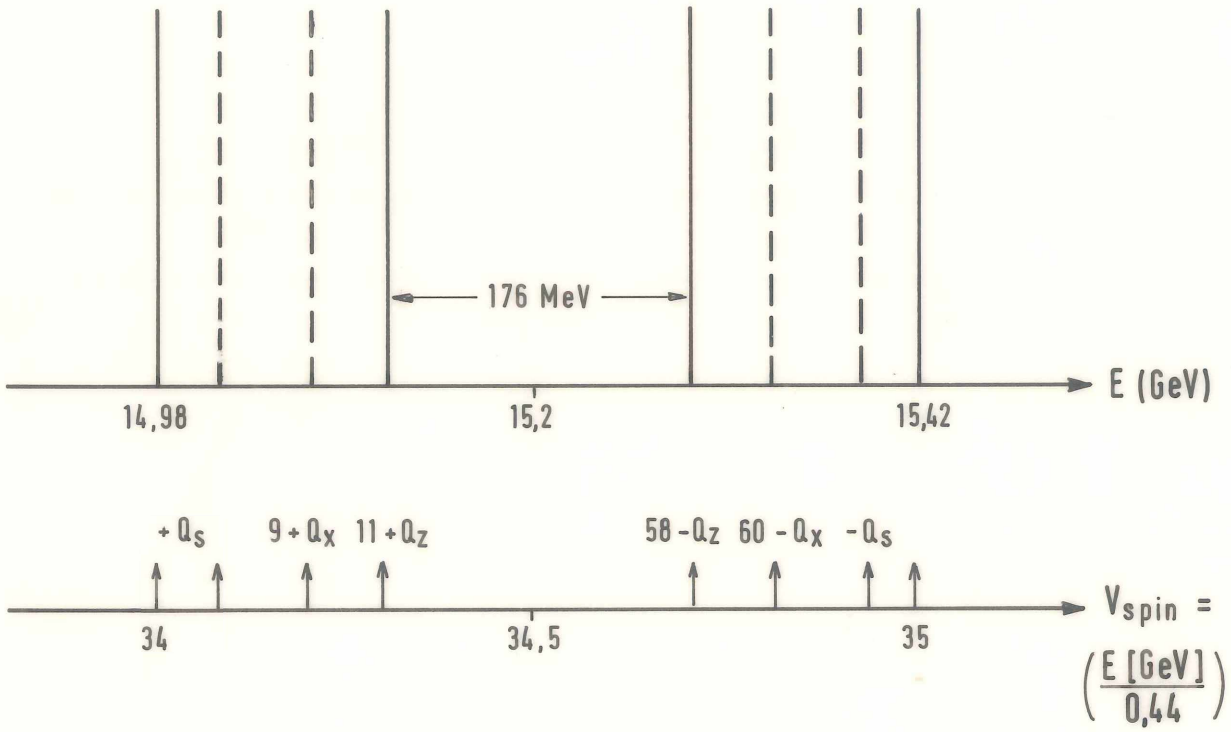
176 MeV
E (GeV)
14,98
15,2
15,42
+Qs
9+Qx
11+Qz
58-Qz
60-Qx
-Qs
34
34,5
35
Vspin = (E [GeV] / 0,44)

fig. 10

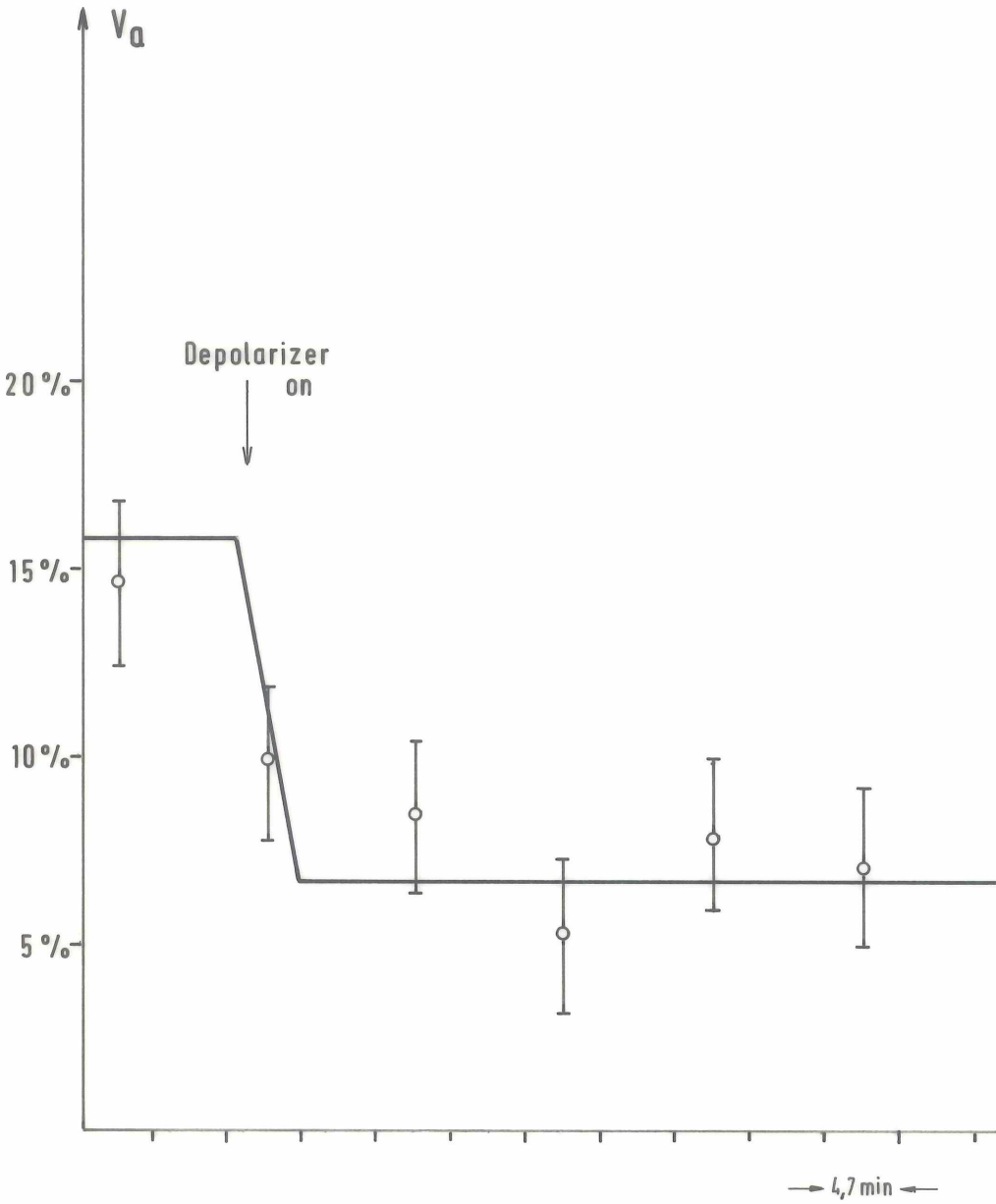

fig. 11

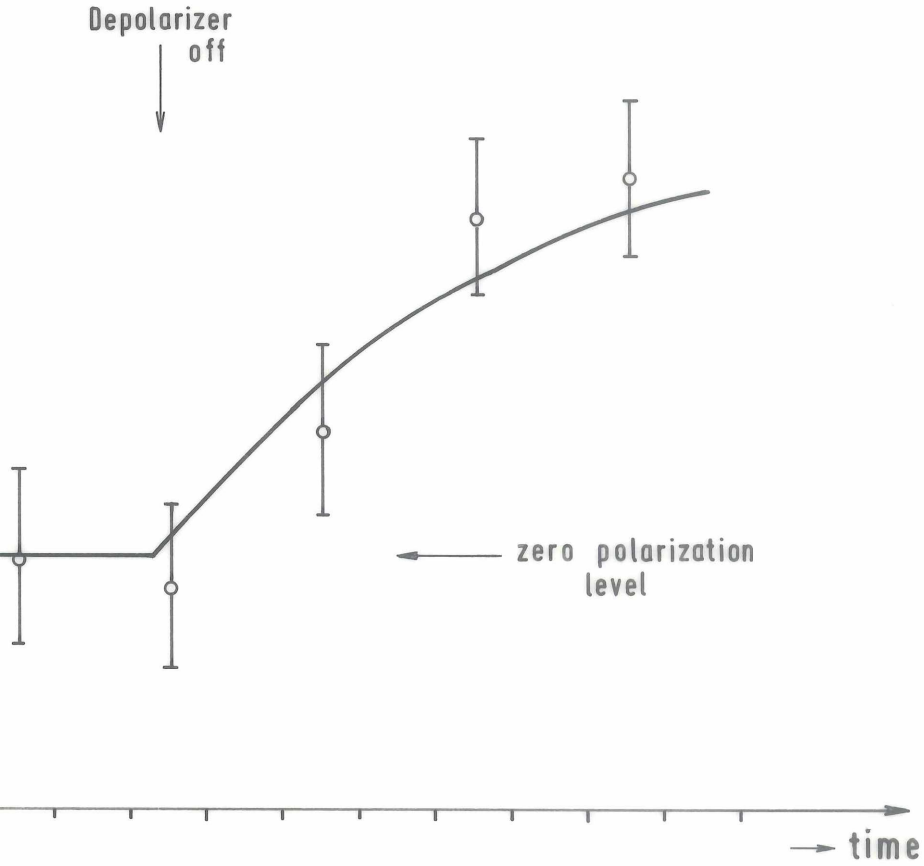
Depolarizer
off
zero polarization
level
time